PHYSICAL REVIEW B **72**, 140102(R) (2005)

Atomistic treatment of depolarizing energy and field in ferroelectric nanostructures

I. Ponomareva, I. I. Naumov, I. Kornev, Huaxiang Fu, and L. Bellaiche
Department of Physics, University of Arkansas, Fayetteville, Arkansas 72701, USA
(Received 11 August 2005; revised manuscript received 22 September 2005; published 24 October 2005)

An *atomistic* approach allowing an accurate and efficient treatment of depolarizing energy and field in *any* low-dimensional ferroelectric structure is developed. Application of this approach demonstrates the limits of the widely used continuum model (even) for simple test cases. Moreover, implementation of this approach within a first-principles-based model reveals an unusual phase transition—from a state exhibiting a spontaneous polarization to a phase associated with a toroid moment of polarization—in a ferroelectric nanodot for a critical value of the depolarizing field.

DOI: 10.1103/PhysRevB.72.140102 PACS number(s): 77.22.Ej, 77.80.Bh, 77.84.Dy

Ferroelectric nanostructures (FEN) are of increasing technological and fundamental interest because of the need in miniaturization of devices, as well as, the appearance of new phenomena (see, e.g., Refs. 1–6, and references therein). Unscreened polarization-induced charges at the surfaces of FEN generate a depolarizing field that is responsible for striking properties. Examples are the existence of a critical thickness below in which no ferroelectricity can appear,[3] and the observation and prediction of laminar stripe nanodomains[2,4] as well as the formation of polarization vortex.[5,6] Interestingly, and despite its huge importance, we are not aware of any model being able to *exactly* calculate the depolarizing field and energy in *any* low-dimensional ferroelectric. For instance, the widely used continuum model (1) neglects the atomistic nature of materials, (2) is technically applicable only in the limit of large enough systems, and (3) cannot predict the depolarizing energy and/or field in the realistic cases of inhomogeneously polarized samples.

In this report we (i) demonstrate that it is possible to derive a scheme allowing the exact *atomistic* computation of the depolarizing energy and field in any low-dimensional FEN; (ii) use this scheme to check the accuracy of the continuum model for some simple test cases; (iii) report an unusual phase transition between two different kinds of order parameters in a ferroelectric nanodot that is driven by the depolarizing field.

To calculate the depolarizing energy in low-dimensional ferroelectrics, one first needs to realize that a system under perfect open-circuit (OC) electrical boundary conditions exhibits a *maximum* depolarizing field (if the polarization lies along a nonperiodic direction), while ideal short-circuit (SC) electrical boundary conditions leads to a complete screening of charges at the FEN surfaces that fully annihilates any depolarizing field. As a result, the depolarizing energy and field experienced by the FEN should involve a *difference* between the dipole-dipole interactions associated with these two extreme electrical boundary conditions. We shall write the energy of the dipole-dipole interaction in *any* system in the form

$$\mathcal{E}_{dip}^{(D)} = \frac{1}{2V}\sum_{\alpha\beta,ij} Q_{\alpha\beta,ij}^{(S,D)} p_\alpha(\mathbf{r}_i) p_\beta(\mathbf{r}_j), \tag{1}$$

where $D=3,2,1$ stands for a system periodic in 3, 2, and 1 directions, respectively; $D=0$ corresponds to nonperiodic systems, and the sum runs over the atomic sites i and j that differ from each other and belong to a *supercell* (to be denoted by S) mimicking the system. Such a supercell is infinitely repeated along the periodic directions, if any. For instance, thin films are modeled by supercells that are repeated in two dimensions while the direction associated with the growth direction of the film is nonperiodic. For dots, the supercell is not repeated. V is the volume of the supercell, $\boldsymbol{p}(\boldsymbol{r}_i)$ the dipole moment at the site i, and $\alpha=x,y,z$ denotes the Cartesian components. The quantity $Q^{(S,D)}$ depends on both the chosen supercell (S) and the periodicity of the system (D).

The elements of the Q matrix for systems periodic in three,[7] two (x and y), one (z) directions[22] and nonperiodic systems are given by

$$Q_{\alpha\beta,ij}^{(S,3)} = \frac{4\pi}{V}\sum_{\mathbf{G}\neq 0}\frac{1}{G^2}\exp\left(-\frac{G^2}{4\lambda^2}\right)G_\alpha G_\beta \cos(\mathbf{G}\cdot\mathbf{r}_{ij}) - \frac{4\lambda^3\delta_{\alpha\beta}\delta_{ij}}{3\sqrt{\pi}},$$

$$Q_{\alpha\beta,ij}^{(S,2)} = \frac{2\pi}{A}\sum_{\mathbf{G}}\left\{G\cos(\mathbf{G}\cdot\boldsymbol{\rho}_{ij})\left[\frac{1}{\sqrt{4\pi}}\Gamma\left(-\frac{1}{2},\frac{G^2}{4\lambda^2}\right)\delta_{\alpha z}\delta_{\beta z} + \frac{1}{G^2}\operatorname{erfc}\left(\frac{G}{2\lambda}\right)G_\alpha G_\beta\right] + G\exp(-G|z_{ij}|)\left[\left(\frac{G_\alpha G_\beta}{G^2} - \delta_{\alpha z}\delta_{\beta z}\right)\cos(\mathbf{G}\cdot\boldsymbol{\rho}_{ij}) - \frac{G_\alpha\delta_{\beta z}}{G}\sin(\mathbf{G}\cdot\boldsymbol{\rho}_{ij})\frac{z_{ij}}{|z_{ij}|}\right]\right\} - \frac{4\lambda^3\delta_{\alpha\beta}\delta_{ij}}{3\sqrt{\pi}},$$

$$Q_{\alpha\beta,ij}^{(S,1)} = \frac{2}{a}\sum_{\mathbf{G}} G^2\cos(\mathbf{G}\cdot z_{ij})\left\{K_0(G\rho_{ij})\delta_{\alpha z}\delta_{\beta z} + \frac{\delta_{\alpha x}\delta_{\beta x}+\delta_{\alpha y}\delta_{\beta y}}{G\rho_{ij}}K_1(G\rho_{ij}) - \frac{1}{\rho_{ij}^2}K_2(G\rho_{ij})\rho_{\alpha,ij}\rho_{\beta,ij}\right\} - \frac{2}{a}\sum_{\mathbf{G}} G\sin(\mathbf{G}\cdot z_{ij})K_1(G\rho_{ij})\rho_{ij}^{-1}G_\alpha\rho_{\beta,ij} + \frac{1}{a^3}(\delta_{\alpha x}\delta_{\beta x}$$

$$+ \delta_{\alpha y}\delta_{\beta y} - 2\delta_{\alpha z}\delta_{\beta z}) \sum_{n=-\infty}^{\infty}{}' \left| n + \frac{z_{ij}}{a} \right|^{-3},$$

$$Q^{(S,0)}_{\alpha\beta,ij} = \delta_{\alpha,\beta}/r^3_{ij} - 3r_{\alpha,ij}r_{\beta,ij}/r^5_{ij}, \qquad (2)$$

where $\mathbf{G}$ are the reciprocal lattice vectors associated with the S supercell, and λ is the Ewald parameter.[8] [Practically, we use $\lambda \sim 2|G_{max}|$ with G_{max} being the reciprocal vectors having the highest magnitude in the summations appearing in Eq. (2)]. δ_{ij} is the Kronicker symbol, A is the supercell area, $\boldsymbol{\rho}_{ij}$ and $\boldsymbol{z}_{ij}$ are the projections of $\boldsymbol{r}_{ij}$ (vector connecting atomic sites i and j) on the $\{x,y\}$ plane and z axis, respectively (i.e., $\boldsymbol{r}_{ij}=\boldsymbol{\rho}_{ij}+\boldsymbol{z}_{ij}$), $\rho_{ij}=|\boldsymbol{\rho}_{ij}|$, and z_{ij} is the component of the $\boldsymbol{z}_{ij}$ vector along the z axis. Γ is the incomplete gamma function and erfc is the complementary error function, a is the supercell length in the z direction; K_n are the modified Bessel's functions. (Note that contributions from $z_{ij}=0$ in $Q^{(S,2)}_{\alpha\beta,ij}$ and contributions from $\rho_{ij}=0$ in $Q^{(S,1)}_{\alpha\beta,ij}$ should be excluded, and that the prime in the right side of $Q^{(S,1)}_{\alpha\beta,ij}$ indicates that the term $n=0$ has to be excluded when $i=j$).

The dipolar interactions described by Eqs. (1) and (2) correspond to *ideal OC conditions* since no charge screening is taken into account in their derivation. The next question to be addressed is what is the dipole-dipole energy in FEN under *perfect SC conditions*? Such energy is simply the one described by the $D=3$ Q matrix. One can justify such a fact by (at least) the three following ways: The first justification is that a ferroelectric nanostructure under short-circuit conditions experiences no depolarizing field, exactly like the infinitely extended (i.e., bulk) systems. Secondly, one can first schematically draw dipoles inside a ferroelectric nanostructure, and then use the so-called image method to impose short-circuit conditions to that nanostructure. The resulting dipole pattern fills all of the three-dimensional space and is identical to the one in the infinite bulk. Finally, the third proof is a practical one and will be seen later, namely that our atomistic predictions using the $D=3$ Q matrix for short-circuit conditions agree with the continuum approach for computation of depolarizing fields in thick-enough nanostructures.

The $\mathcal{E}^{(D)}_{dep}$ (maximum) depolarizing energy per volume in any FEN can now easily be calculated as the difference in dipole-dipole energies between perfect OC and SC conditions, that is

$$\mathcal{E}^{(D)}_{dep} = \mathcal{E}^{(D)}_{dip} - \mathcal{E}^{(3)}_{dip} = \frac{1}{2V}\sum_{\alpha\beta,ij}[Q^{(S,D)}_{\alpha\beta,ij} - Q^{(S,3)}_{\alpha\beta,ij}]p_\alpha(\mathbf{r}_i)p_\beta(\mathbf{r}_j) \qquad (3)$$

where the sum over i and j run over the sites of the chosen supercell of the FEN, and where $Q^{(S,D)}_{\alpha\beta,ij}$ are given by Eq. (2). Equation (3) is, to the best of our knowledge, the first proposed form allowing an atomistic and exact computation of depolarizing energy in *any* FEN with *any* dipole distribution. (Note that such form can also be applied to calculate demagnetization energy in low-dimensional *magnetic* systems.)

We first apply our approach to compute $\mathcal{E}^{(D)}_{dep}$ in some *test* cases. Here, we limit ourselves to systems adopting a simple cubic structure in which each atomic site has a local and equal-in-magnitude dipole moment. Note that all of the results to be reported here do not depend on the size used for the periodic direction(s) of the S supercell.

Homogeneous dipole distribution. Let us first investigate FEN exhibiting the same local dipole $\mathbf{p}$ at any atomic site. We shall present our results in the form of $\mathcal{E}^{(D)}_{dep} = \gamma\mathcal{E}^{(D,cont)}_{dep}$, where $\mathcal{E}^{(D)}_{dep}$ is obtained from Eq. (3), while $\mathcal{E}^{(D,cont)}_{dep}$ is the depolarizing energy predicted by the continuum model. γ is thus a "correcting" coefficient that provides a measure of the continuum approach accuracy.

For (001) ultrathin films homogeneously polarized along the out-of-plane (z) direction, the continuum model predicts that $\mathcal{E}^{(2,cont)}_{dep} = 2\pi P^2$, independently of the film thickness, where P is the polarization. On the other hand, the use of Eq. (3) results in $\gamma = 1.017$, 1.010, 1.007, and 1.006 for ultrathin films of 3, 5, 7, and 9 layers, respectively. In other words, our atomistic approach reveals that the depolarizing energy is slightly larger than the one predicted by the continuum model and increases as the number of film layers decreases. Such findings are consistent with those of Refs. 9–11. To understand them, we rewrite Eq. (3) in the case of a *homogeneous* dipole pattern as follows:

$$\mathcal{E}^{(D)}_{dep} = \frac{p_\alpha p_\beta}{2V}\sum_{\alpha\beta,j} F^{(D)}_{\alpha\beta}(j), \quad \text{with } F^{(D)}_{\alpha\beta}(j) = \sum_i [Q^{(S,D)}_{\alpha\beta,ij} - Q^{(S,3)}_{\alpha\beta,ij}] \qquad (4)$$

Figure 1(a) shows the "depolarizing" factors $\langle F^{(D=2)}_{zz}(l)\rangle$ averaged over all the j sites belonging to a given (00l) layer (that is indexed by l) for our films, as a function of a layer position inside the film. Comparison with its continuum predicted (and l-independent) value of 4π is also given. Figure 1(a) clearly reveals that the deviation of the continuum model from our atomistic results is confined to the surface layers—as also found in Ref. 11—and that this deviation is an underestimation. (Note that such surface effects can be qualitatively important, e.g., they can lead to *asymmetric* temperature-versus-misfit-strain phase diagram.[12]) This explains why we numerically found that the $\mathcal{E}^{(2)}_{dep}$ increases with respect to the continuum prediction as the film becomes thinner, since the ratio of surface layers over total layers increases as the film thickness decreases. Figure 1(a) also shows that for the surface layers $\langle F^{(2)}_{xx}\rangle = \langle F^{(2)}_{yy}\rangle$ are negative—as discussed in Ref. 10—and that $1 + (\langle F^{(2)}_{xx}\rangle - \langle F^{(2)}_{zz}\rangle)/4\pi = -0.0393$, which is in perfect agreement with the calculation of the so-called surface anisotropy in Ref. 11. (Note that the surface anisotropy is null in the continuum model framework.)

We next consider different wires of square cross sections, that are periodic along the z direction and homogeneously polarized along the x axis. According to the continuum approach, such wires should have a depolarizing energy $\mathcal{E}^{(1,cont)}_{dep} = \pi P^2$, independently of the wire thickness. We numerically found via Eq. (3) that $\gamma = 1.017$, 1.010, 1.007, and 1.006 for wires of 3, 5, 7, and 9 shells, respectively [see inset of Fig. 1(b) for definition of shells]. Like in the films, the continuum model underestimates the depolarizing energy and this underestimation becomes larger in magnitude as the

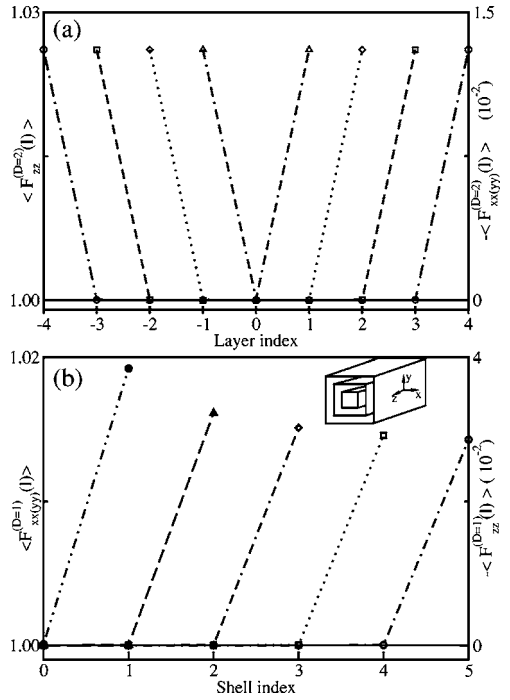

FIG. 1. Depolarizing factors $\langle F_{xx}^{(D)}(l)\rangle$, $\langle F_{yy}^{(D)}(l)\rangle$, and $\langle F_{zz}^{(D)}(l)\rangle$ obtained with our atomistic approach and normalized to 4π (that is the prediction of F_{zz} in the continuum model) in the case of (001) films [(a)] and 2π (prediction of F_{xx} in the continuum model) in the case of wires periodic along the z axis [(b)] as a function of the layer or shell index l. The different shells of a wire are shown in the inset of part (b). The most inner layer or shell is indexed by 0. The different symbols correspond to different thicknesses.

nanostructure shrinks in size. Figure 1(b) shows that the continuum model fails to reproduce the averaged depolarizing factor for the surface shell but exactly agrees with our atomistic results for all the inner shells.

We now turn our attention to a cubic dot homogeneously polarized along the z direction. Unlike the previous two cases, our atomistic approach gives a depolarizing energy that is not only independent on the dot size but also exactly agrees with the continuum approach (that is, $\mathcal{E}_{dep}^{(0)}=\mathcal{E}_{dep}^{(0,cont)}=2\pi P^2/3$). Such a surprising result is caused by the sum rule[10] for depolarization factors (that is, $F_{xx}+F_{yy}+F_{zz}$ is the constant given by the continuum model) that we numerically found to be valid in *every* layer (shell) of any system investigated so far (i.e., films, wires and dots). Moreover, cubic dots exhibit x, y, and z directions that are symmetrically equivalent (which is not the case in wires and thin films). As a result, $\langle F_{xx}^{(D)}(l)\rangle=\langle F_{yy}^{(D)}(l)\rangle=\langle F_{zz}^{(D)}(l)\rangle$ in dots. Because of the sum rule, each of these factors is equal to the continuum prediction of $4\pi/3$ for any shell and for any size, and the continuum model predicts the right depolarizing energy.

Inhomogeneous dipole distribution. Let us now investigate 2D, 1D, and 0D FEN exhibiting stripe domains with the dipoles assumed to be homogeneous inside each domain (with a p magnitude) and perpendicular to a periodic direction, if any (see the inset of Fig. 2). The period of stripe domains is denoted as d. The $\mathcal{E}_{dep}^{(D)}$ energy calculated from Eq. (3) for a film having a thickness $L=10$ atomic layers is

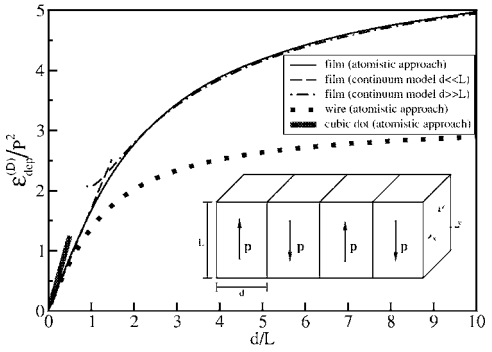

FIG. 2. Normalized depolarization energy as a function of d/L for quasi 0D, 1D, and 2D systems with stripe domains along with continuum model prediction (Refs. 13 and 15) for $d\ll L$ and $d\gg L$ for $D=2$ systems. The inset shows the schematic representation of the chosen polarization pattern in (001) films, or wires periodic along y or cubic dots.

shown as a function of d/L in Fig. 2, along with depolarization energies calculated in the continuum approach for the two limiting cases[13–15] $d\ll L$ (i.e., $\mathcal{E}_{dep}^{(2,cont)}=1.7P^2d/L$) and $d\gg L$. One can see that these two limiting cases can reproduce rather well the energy derived from Eq. (3) for $d/L<1$ and $d/L>2$, respectively. Furthermore we numerically found that our depolarization energy can be parametrized as following:

$$\mathcal{E}_{dep}^{(D)}=[c_0(1-c_1e^{-d/c_2L})+(n\pi-c_0)(1-e^{-d/c_3L})]P^2, \quad (5)$$

where $c_0=2.568$, $c_1=1.024$, $c_2=14.118$, $c_3=1.831$, $n=2$.

Figure 2 also reports our results for two cases in which we are not aware of any continuum predictions, namely stripe domains in infinite wires and cubic dots. Note that the stripe direction is along the wire y periodic direction and that the *finite* size of 0D systems implies that d/L has a maximum value of 0.5 in cubic dots. We present here results for a wire of 10 shells (10×10 atomic sites for cross section) and for a cubic dot of 10 shells ($10\times10\times10$ atomic sites) with d ranging from 1 to 5 atomic layers. Two features seen in Fig. 2 are particularly striking. First of all, the stripe domains have less depolarizing energy in a wire than in a thin film for the same d/L, with this difference becoming more pronounced as d/L increases. The parameters of Eq. (5) for the wire are $c_0=2.208$, $c_1=1.000$, $c_2=1.196$, $c_3=7.398$, and $n=1$. Secondly, for the case of a cubic dot, the dependence of depolarizing energy on d/L is linear and given by $\mathcal{E}_{dep}^{(0)}=2.5P^2d/L$.

We finally take advantage of our formalism to reveal, from realistic first-principles-based calculations, properties of a free-standing $Pb(Zr_{0.4}Ti_{0.6})O_3$ (PZT) cubic dot of 48 Å lateral size for different electrical boundary conditions. The total energy of the system used in Monte Carlo simulations is:

$$\mathcal{E}_{Heff}[\mathbf{p}(\mathbf{r}_i),\mathbf{v}_i,\eta,\sigma_i]+\beta\sum_i\langle\mathbf{E}_{dep}\rangle\cdot\mathbf{p}(\mathbf{r}_i), \quad (6)$$

where $\mathcal{E}_{Heff}$ is the (first-principles-derived effective Hamiltonian) energy for PZT (Ref. 16) which is dependent on the

$\mathbf{p}(\mathbf{r}_i)$ local dipoles at site i of the dot, the $\mathbf{v}_i$ inhomogeneous strain related variables, the η homogeneous strain tensor, and on the σ_i atomic configuration.[16] The dipole-dipole interactions in this H_{eff} are given by the Q matrix with $D=0$ of Eq. (2). The second term of Eq. (6) mimics a screening of the (maximum) depolarizing field, with the magnitude of this screening being controlled by the β coefficient. $\beta=1$ and $\beta=0$ corresponds to ideal SC and OC electrical boundary conditions, respectively, while a value of β in-between corresponds to more realistic electrical situation.[3] $\langle \mathbf{E}_{dep} \rangle = -(1/N\epsilon_\infty)\Sigma_j[\partial \mathcal{E}_{dep}^{(D=0)}/\partial \mathbf{p}(r_j)]$ is the maximum depolarizing field inside the dot, while N and ϵ_∞ are the total number of sites of the dot and the dielectric constant of PZT, respectively. $\mathcal{E}_{dep}^{(D=0)}$ is practically calculated from Eq. (3).

Figures 3(a) and 3(b) show the resulting macroscopic dipole moment and the macroscopic toroid moment of polarization (i.e., the supercell average of the cross product between position and dipole moment[6]), respectively, as a function of β. One can clearly see that for situations close to SC, the dot exhibits a macroscopic *polarization*, with a cross section of the local dipole pattern being given in the inset of Fig. 3(a) and bearing resemblence with the so-called flower state found in small magnetic dots.[17] On the other hand a dot with electrical boundary conditions close to OC has a nonvanishing *toroid moment*,[6] with a cross section of the corresponding dipole pattern being displayed in the inset of Fig. 3(b) and looking like the so-called vortex or curling state exhibited by magnetic dots above a certain size.[17] Moreover, Fig. 3 clearly reveals that, at a critical value of the depolarization field, the system undergoes an unusual phase transition between a state characterized by one kind of order parameter (toroid moment of polarization) to a state associated with another kind of order parameter (polarization).[23] In other words, no coexistence between these two order parameters occurs—most likely to avoid a simultaneous cost in electrostatic energy (via the depolarizing field that would exist if the dot exhibits a spontaneous polarization) *and* short-range interactions (because of the large dipoles inhomogeneities associated with a spontaneous toroid moment).

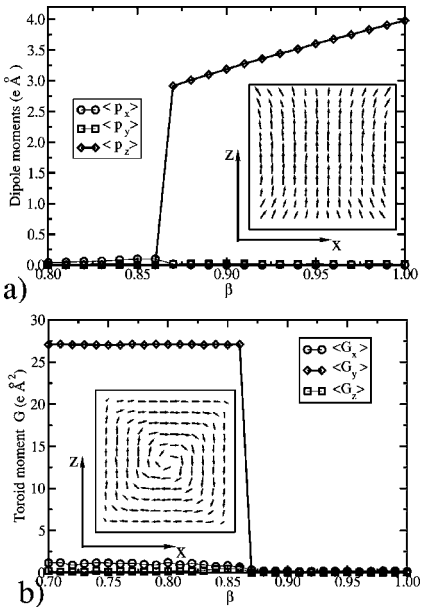

FIG. 3. (a) Dipole moments and (b) toroid moments of polarization G in a PZT nanodot as a function of the screening coefficient β. Insets of (a) and (b) show the polarization pattern for $\beta=1$ (SC conditions) and $\beta=0$ (OC conditions), respectively.

In summary, we have derived an *atomistic*, simple, general, and efficient approach to calculate the depolarizing energy and field in *any* low-dimensional ferroelectric structure. The application of this method reveals—and explains—the limits of the continuum model, and also results in the discovery of an unusual phase transition in a ferroelectric dot for some critical value of the residual depolarizing field.

We thank P. Ghosez for discussion. This work was supported by NSF Grant Nos. DMR-0404335 and DMR-9983678, by ONR Grant Nos. D 00014-01-1-0365, D 00014-04-1-0413, and D 00014-01-1-0600 and by DOE Grant No. DE-FG02-05ER46188.

[1] J. F. Scott and C. A. P. de Araujo, Science **246**, 1400 (1989).
[2] D. Fong *et al.*, Science **304**, 1650 (2004).
[3] J. Junquera and P. Ghosez, Nature (London) **422**, 506 (2004).
[4] I. Kornev *et al.*, Phys. Rev. Lett. **93**, 196104 (2004).
[5] H. Fu and L. Bellaiche, Phys. Rev. Lett. **91**, 257601 (2003).
[6] I. I. Naumov *et al.*, Nature (London) **432**, 737 (2004).
[7] W. Zhong *et al.*, Phys. Rev. B **52**, 6301 (1995).
[8] C. Kittel, *Introduction to Solid State Physics*, 7th ed. (John Wiley and Sons, New York, 1996), pp. 386–388.
[9] P. J. Jensen, Ann. Phys. **6**, 317 (1997).
[10] E. Vedemenko *et al.*, J. Magn. Magn. Mater. **256**, 237 (2003).
[11] H. Draaisma and W. de Jonge, J. Appl. Phys. **64**, 3610 (1988).
[12] B.-K. Lai *et al.*, Appl. Phys. Lett. **86**, 132904 (2005).
[13] C. Kittel, Phys. Rev. **70**, 965 (1946).
[14] T. Mitsui and H. Furuichi, Phys. Rev. **90**, 193 (1953).
[15] B. Kaplan and G. Gehring, J. Magn. Magn. Mater. **128**, 111 (1993).
[16] L. Bellaiche *et al.*, Phys. Rev. Lett. **84**, 5427 (2000).
[17] A. Hubert and R. Schafer, *Magnetic Domains* (Springer, New York, 2000), pp. 167–168.
[18] I. Naumov and H. Fu, cond-mat/0505497 (unpublished).
[19] Y. J. Rhee *et al.*, Phys. Rev. B **40**, 36 (1989).
[20] A. Brodka, Chem. Phys. Lett. **363**, 604 (2002).
[21] A. Brodka and A. Grzybowski, J. Chem. Phys. **117**, 8208 (2002).
[22] To calculate the elements of the Q matrix we developed an original approach using *periodic* Green's function—satisfying Laplace equation and *analytically* determined. Details of this approach are given in Ref. 18. Note that other approaches allowing the calculation of dipolar interactions can be found in Refs. 9 and 19–21.
[23] Some subtle effects near the surface (such as modification of the electronic structure or surface relaxation) have been neglected here since Ref. 5 showed that they negligeably affect properties of ferroelectric dots. For instance, incorporating surface relaxations, as in Ref. 5, leads to the same critical value of β for the transition depicted in Fig. 3.